Cyan and Yellow Super Fluorescent Proteins with Improved Brightness, Protein Folding, and FRET Förster Radius[†,‡]

Gert-Jan Kremers, Joachim Goedhart, Erik B. van Munster, and Theodorus W. J. Gadella, Jr.*

Section Molecular Cytology and Centre for Advanced Microscopy, Swammerdam Institute for Life Sciences, University of Amsterdam, Kruislaan 316, 1098 SM, Amsterdam, The Netherlands

Received August 16, 2005; Revised Manuscript Received March 29, 2006

ABSTRACT: Enhanced cyan and yellow fluorescent proteins are widely used for dual color imaging and protein−protein interaction studies based on fluorescence resonance energy transfer. Use of these fluorescent proteins can be limited by their thermosensitivity, dim fluorescence, and tendency for aggregation. Here we report the results of a site-directed mutagenesis approach to improve these fluorescent proteins. We created monomeric optimized variants of ECFP and EYFP, which fold faster and more efficiently at 37 °C and have superior solubility and brightness. Bacteria expressing SCFP3A were 9-fold brighter than those expressing ECFP and 1.2-fold brighter than bacteria expressing Cerulean. SCFP3A has an increased quantum yield (0.56) and fluorescence lifetime. Bacteria expressing SYFP2 were 12 times brighter than those expressing EYFP(Q69K) and almost 2-fold brighter than bacteria expressing Venus. In HeLa cells, the improvements were less pronounced; nonetheless, cells expressing SCFP3A and SYFP2 were both 1.5-fold brighter than cells expressing ECFP and EYFP(Q69K), respectively. The enhancements of SCFP3A and SYFP2 are most probably due to an increased intrinsic brightness (1.7-fold and 1.3-fold for purified recombinant proteins, compared to ECFP & EYFP(Q69K), respectively) and due to enhanced protein folding and maturation. The latter enhancements most significantly contribute to the increased fluorescent yield in bacteria whereas they appear less significant for mammalian cell systems. SCFP3A and SYFP2 make a superior donor−acceptor pair for fluorescence resonance energy transfer, because of the high quantum yield and increased lifetime of SCFP3A and the high extinction coefficient of SYFP2. Furthermore, SCFP1, a CFP variant with a short fluorescence lifetime but identical spectra compared to ECFP and SCFP3A, was characterized. Using the large lifetime difference between SCFP1 and SCFP3A enabled us to perform for the first time dual-lifetime imaging of spectrally identical fluorescent species in living cells.

Since the cloning of the green fluorescent protein (GFP)[1] gene from the jellyfish *Aequorea victoria* (*1*, *2*), mutagenesis of GFP has generated a variety of visible fluorescent proteins (VFPs) with fluorescence ranging from blue to greenish-yellow (*3*). Besides mutations that affect the spectral properties, numerous modifications have been described that improve the brightness of one or more VFP variants. Such mutations can act in different ways, for example by improving chromophore formation (F64L, V68L), protein folding (S72A, V163A, S175G), and solubility (M153T, V163A) (*4*−*8*).

Enhanced cyan (ECFP) and enhanced yellow (EYFP) fluorescent proteins are widely used, since they can be applied for dual color imaging and for fluorescence resonance energy transfer (FRET) applications to study protein−protein interaction (*9*, *10*). Unfortunately, ECFP is about 4 times less bright than EYFP, because of lower absorbance and fluorescence quantum yield. Therefore, improving ECFP fluorescence would facilitate visualization of CFP-fusion proteins and enable higher FRET efficiencies for CFP and YFP.

The FRET efficiency (E) of a donor−acceptor pair is dependent on the average distance (r) between donor and acceptor and on the Förster radius (R_0) as defined by Förster's theory (*11*),

$$E = \frac{1}{1 + (r/R_0)^6} \tag{1}$$

in which R_0 is the distance at which 50% FRET occurs. R_0 can be calculated from the equation (*11*, *12*)

$$R_0^{\,6} = c\kappa^2\eta^{-4}\varphi_d\epsilon_a J(\lambda) \tag{2}$$

where c is 8.786×10^{-11} mol L^{-1} cm nm^2, κ^2 the orientation

[†] This work was supported by the European Union integrated project on Molecular Imaging (LSHG-CT-2003-503259). Part of this work was enabled through Vernieuwingsimpuls Grant 016.001.024 (T. den Blaauwen, University of Amsterdam, Amsterdam, The Netherlands) from The Netherlands Organization for Scientific Research (NWO).

[‡] The nucleotide sequences of all SVFP variants have been deposited in the GenBank database under GenBankAccession Numbers DQ092360 (mVenus), DQ092361 (SYFP2), DQ092362 (SCFP1), DQ092363 (SCFP2), DQ092364 (SCFP3A), and DQ092365 (SCFP3B).

* To whom correspondence should be addressed. Tel: +31 20 525 6259. Fax: +31 20 525 7934. E-mail: Gadella@science.uva.nl.

[1] Abbreviations: AU, arbitrary units; CFP, cyan fluorescent protein; DTT, dithiothreitol; ECFP, enhanced cyan fluorescent protein; EYFP, enhanced yellow fluorescent protein; FLIM, fluorescence lifetime imaging microscopy; FRET, fluorescence resonance energy transfer; GFP, green fluorescent protein; GST, glutathione S-transferase; IPTG, isopropyl-β-D-thiogalactopyranoside; NES, nuclear export sequence; NLS, nuclear localization sequence; OD, optical density; PMSF, phenylmethylsulfonyl fluoride; QY, fluorescence quantum yield; VFP, visible fluorescent protein; YFP, yellow fluorescent protein.

10.1021/bi0516273 CCC: $33.50
Published on Web 05/03/2006

factor of the interacting dipoles, η the refractive index of the medium separating donor and acceptor chromophore, φ_d the quantum yield of the donor, ϵ_a the extinction coefficient of the acceptor with dimensions mol^{-1} L cm^{-1}, and $J(\lambda)$ the overlap integral. Generally, κ^2 is set to 2/3, which is true if donor and acceptor are rapidly randomly orientated (*13*−*15*), and then R_0 is dependent only on φ_d, ϵ_a, and $J(\lambda)$. When comparing donor−acceptor pairs with identical absorbance and emission spectra, $J(\lambda)$ is identical and the difference in R_0 is directly related to φ_d and ϵ_a. From eqs 1 and 2 it can be derived that, in the case in which the average distance between donor and acceptor is also constant, the FRET efficiencies of donor−acceptor pair E and S are related according to

$$E_s = \frac{Y}{\frac{1}{E_e} - 1 + Y} \quad (3)$$

with E_s the FRET efficiency of pair S, E_e the efficiency of pair E, and Y defined as

$$Y = \frac{(\varphi_d \epsilon_a)_S}{(\varphi_d \epsilon_a)_E} \quad (4)$$

Our strategy to improve ECFP was based on Venus, a recently described improved YFP variant (*16*). Venus matures much faster and more efficiently than EYFP at 37 °C, because of one novel YFP-specific mutation (F46L) and four common folding mutations (F64L, M153T, V163A, and S175G) that have not been used together in EYFP before. More recently, also a bright ECFP variant named Cerulean was described, with improved extinction coefficient and fluorescence quantum yield, as a result of 2 mutations, Y145A and H148D (*17*). An additional feature of Cerulean is a fluorescence lifetime decay best fitted by a single exponential. We have studied whether ECFP fluorescence would also benefit from these mutations. Since ECFP already contains the folding mutations F64L, M153T, and V163A, we concentrated on the remaining mutations. In addition, the effects of V68L and A206K both in ECFP and in Venus were studied. A206K has been described to abolish the tendency of YFP to dimerize (*18*). Because of their improved folding and brightness, we named these VFP variants Super Fluorescent Proteins or SCFPs and SYFPs, respectively, to indicate the upgrade from the well-known, enhanced fluorescent proteins ECFP and EYFP. Besides detailed spectroscopic characterization, expression of VFPs was studied in *Escherichia coli* bacteria and in mammalian cells, and the FRET efficiency of YFP−CFP heterodimers was determined.

EXPERIMENTAL PROCEDURES

Construction of VFP Vectors. All vectors were made using standard molecular biological methods (*19*). VFP variants were obtained by site-directed mutagenesis using the QuickChange site-directed mutagenesis kit (Stratagene, La Jolla, CA) or a modified version of this protocol (*20*). The modified protocol used a combination of 5′-phosphorylated oligonucleotides and ligation during amplification, enabling the incorporation of multiple mutations at once. A list of oligonucleotides used for mutagenesis is shown in Table S1 (Supporting Information).

For bacterial expression VFPs were cloned into plasmid pGEX-MCS. pGEX-MCS was created by inserting a modified multiple cloning site as a *Bam*HI/*Hin*DIII fragment into pGEX-KG (*21*). The modified multiple cloning site consisted of 2 annealing oligonucleotides 5′-GATCTACCATGGAATTCAGCGGCCGCTCTAGAGGATCCA-3′ and 5′-AGCTTGGATCCTCTAGAGCGGCCGCTGAATTCCATGGTA-3′ with 5′ overhangs compatible with *Bam*HI and *Hin*DIII restriction sites. The *Bam*HI site was disrupted by a C>T modification immediately after the 5′ overhang. pGEX-EYFP(Q69K) was made by inserting EYFP(Q69K) (human codon-optimized wtGFP with S65G, V68L, Q69K, S72A, and T203Y) from pMON999d35S-YFP (*22*) as a *Nco*I/*Xba*I fragment into pGEX-MCS. pGEX-ECFP was formed by inserting ECFP (human codon-optimized wtGFP with F64L, S65T, Y66W, N146I, M153T, and V163A) from pECFP-N1 (Clontech, Palo Alto, CA) as a *Nco*I/*Not*I fragment into pGEX-MCS. pGEX-Venus was made by inserting Venus (EYFP with F46L, F64L, M153T, V163A, and S175G) from pCS2+ Venus (a generous gift of A. Miyawaki) into pGEX-MCS as a *Nco*I/*Eco*RI fragment. pGEX-Cerulean(A206K) was created by inserting Cerulean(A206K) from pCerulean(A206K)-C1 (a generous gift of D. W. Piston) as a *Nco*I/*Bsr*GI fragment into pGEX-SCFP2.

Mammalian expression vectors were created in pEGFP-C1 (Clontech) by replacing the EGFP coding sequence. A *Nhe*I restriction site was introduced upstream of the VFP cDNA by polymerase chain reaction (PCR) with primers 5′-CC**GCTAGC**GCTACCGGTCGCCACCATGGTGAGCAAGG-3′ and 5′-CGAGATCTGAGTCCGGACTTGTACAGCTCGTCC-3′, and VFPs were ligated as *Nhe*I/*Bsr*GI fragments.

Mammalian expression vector encoding tandem dimers of YFP and CFP variants were constructed by inserting EYFP-(Q69K) as a *Nhe*I/*Bam*HI fragment into pECFP-N1 (Clontech). The *Bam*HI site was introduced into EYFP(Q69K) immediately downstream of the *Bgl*II site present in pEYFP-(Q69K)-C1 by PCR with primers 5′-AGGTCTATATAAGCAGAGC-3′ (anneals in the CMV promoter) and 5′-AT**GGATCC**GAAGATCTGAGTCCGGACTTG-3′. The other heterodimers were created by replacing EYFP(Q69K) for SYFP2 from vector pSYFP2-C1 (*Nhe*I/*Bgl*II fragment) and replacing ECFP for SCFP3A from vector pSCFP3A-N1 (*Bam*HI/*Bsr*GI fragment).

Plasmid pSCFP3A-NES encoding SCFP3A with a nuclear export sequence (SELQNKLEELDLDSYK; J. Goedhart, unpublished) fused to the C-terminus. Plasmid pSCFP1-NLS encoding SCFP1 with a nuclear localization sequence fused to the C-terminal lysine (GGPKKKRKV; J. Goedhart, unpublished). All constructs were checked by DNA sequencing (Baseclear, Leiden, The Netherlands).

Fluorescent Protein Isolation. Fluorescent proteins were isolated as GST-fusion proteins. Four hundred milliliters of TY-medium (10 g/L bactotryptone, 5 g/L yeast extract, 5 g/L NaCl, and 3 mL/L 1 N NaOH), supplemented with 100 μg/mL ampicillin and 0.4% (w/v) glucose, was inoculated with 8 mL of starter culture, which was grown overnight. Bacteria were grown at 37 °C until $OD_{600} \approx 0.6$ and cooled to room temperature. Protein synthesis was induced with 0.1 mM IPTG (Duchefa Biochemie BV, Haarlem, The Netherlands) for 5 h at 21 °C. Bacteria were washed once with 40 mL of STE (20 mM Tris-HCl, 1 mM EDTA, 150 mM NaCl,

pH 8) and stored at −70 °C until further processing. Bacterial pellets were thawed and resuspended in 10 mL of STE, containing 1 mg/mL lysozyme, 5 mM DTT, 1 mM PMSF, and 0.1% NP-40. Cells were disrupted by sonication. After centrifugation for 30 min at 40000*g*, the supernatant was passed through a 0.22 μm filter and added to 2 mL of 50% glutathione-agarose (Sigma-Aldrich, St. Louis, MO). After 1 h incubation, the glutathione-agarose with GST-tagged protein was washed 3 times with 10 mL of STE, containing 5 mM DTT, 1 mM PMSF, and 0.1% Triton-X100, and 3 times with 10 mL of STE. The GST-tag was removed by incubation overnight with 50 units of thrombin (Amersham Bioscience, Uppsala, Sweden) at room temperature. Samples were desalted over a Sephadex PD10 column using 20 mM Tris-HCl, pH 8.5. Proteins were further purified by ion exchange chromatography using a monoQ column on an ÄKTA FPLC machine (Amersham Bioscience) and a linear NaCl gradient (10 mM/mL, flow 1 mL/min) in 20 mM Tris-HCl, pH 8.5. Fluorescent protein eluted around 250 mM NaCl. Protein concentrations of all fluorescent fractions were determined by the Pierce BCA protein assay (Pierce Biotechnology, Rockford, IL), using a bovine serum albumine standard as reference. Fractions were pooled and spectral grade glycerol (Sigma-Aldrich) was added to 50% (v/v) for long-term storage at minus 20 °C. Sample purity was checked by SDS-PAGE to be >95%.

Spectral Characterization. Spectral measurements were done in 20 mM Tris-HCl, 1 mM EDTA pH 8. Absorbance spectra were measured on a Uvikon293 dual beam spectrophotometer (Bio-Tek Instruments, Winooski, VT). Extinction coefficients were calculated by applying Beer's law on the absorbance spectra obtained from the fractions collected after monoQ FPLC. For each VFP variant up to 3 fractions with different concentrations ($0.1 < OD_{\lambda max} < 1$) of 3 independent protein isolations were used for determining the extinction coefficient. A molar mass of 27 kDa was used for all VFPs. Fluorescence spectra were measured on a PTI QuantaMaster 2000-4 fluorescence spectrofluorometer (Photon Technology International, Lawrenceville, NJ) and corrected for differences in excitation intensity and detector sensitivity. Fluorescence quantum yield measurements were done on diluted VFP solutions from 3 independent protein isolations with similar OD ($OD_{\lambda ex} \leq 0.05$) with fluorescein (Molecular Probes, Eugene, OR) in borate buffer solution pH 9.1 (QY 0.92) (*23*) as quantum yield standard.

pK_a Measurements. For pH titrations, fluorescent protein was diluted to 25−75 nM in wells of a 96-well plate containing 200 μL of titration buffer. Titration buffers contained 50 mM citric acid/Na citrate (pH 3−5.5), KH_2PO_4/Na_2HPO_4 (pH 6−8), or glycine/NaOH (pH 8.5−10). Plates were analyzed using an FL600 fluorescence microplate reader (Bio-Tek Instruments) equipped with custom ordered filters. For YFP and CFP fluorescence, BP485/20 and BP430/25 excitation filters and BP530/25 and BP485/40 emission filters (Chroma Technology Corp., Rockinham, VT) were used, respectively. The pK_a was determined by fitting a sigmoid equation using Igor Pro 5.0 software (Wavemetrix, Portland, OR).

Bleach Measurements. Bleach experiments were performed according to a modified protocol as described by Patterson et al. (*7*). Fifty microliters of fluorescent protein solution (~0.25 μM in 20 mM Tris-HCl, 1 mM EDTA, 5% (v/v) poly(ethylene glycol) 4000, pH 8) was mixed with 450 μL of 1-octanol (Spectral grade, Sigma-Aldrich) and emulsified by passing 15 times through a 25G surgical syringe. Four microliters of the emulsion was put on an object slide and covered with an 18 × 18 mm coverglass. Single microdroplets were bleached under continuous widefield illumination (0.22 $\mu W/\mu m^2$ for CFP and 0.026 $\mu W/\mu m^2$ for YFP) on an Axiovert200M microscope (Zeiss, Jena, Germany) fitted with a Zeiss plan Neofluar 40 × 1.3NA, oil-immersion objective, using a 100 W high pressure Hg lamp for excitation. Repeatedly, the bleach kinetics of a uniform reference layer (*24*) was measured, to verify the intensity of excitation light. Bleach series were recorded on a Coolsnap HQ CCD camera (Roper Scientific, Tucson, AZ). YFP or CFP fluorescence was detected, using HQ500/20 and D436/20 excitation filters, 525DCXR and 455DCLP dichroic mirrors, and HQ545/30 and D480/40 emission filters, respectively (Chroma Technology Corp.). Data analysis was done by fitting a single-exponential decay.

Refolding and Oxidation of Fluorescent Proteins. Refolding studies were performed as described (*25*). Fluorescent protein was denatured by heating for 5 min at 95 °C in the presence of 8 M urea and 1 mM DTT and cooled to room temperature. For chromophore reduction 5 mM sodium-dithionite was added before denaturation. Refolding was initiated by 100-fold dilution in refolding buffer (50 mM Tris-HCl, 35 mM KCl, 2 mM $MgCl_2$, 1 mM DTT, pH 7.5) at 37 °C. Protein refolding and oxidation was followed in time by measuring the recovery of fluorescence while stirring. An equal amount of native protein was used to determine the fluorescence intensity of nondenatured protein. Rate constants for refolding (fast component) and reoxidation (slow component) were obtained by fitting a double-exponential equation.

Localization in E. coli. A 0.5 mL volume of a starter culture which was grown overnight was used to inoculate 25 mL of TY-medium, supplemented with 100 μg/mL ampicillin and 0.4% (w/v) glucose and grown to $OD_{600} \approx 0.6$ at 37 °C. Induction of protein synthesis was initiated upon 10-fold dilution into medium containing 0.1 mM IPTG. After 4 h incubation at 37 °C, cells were fixed with 2.8% formaldehyde/0.04% glutaraldehyde. Microscopy slides were prepared by pipetting bacteria on an object slide containing a thin layer of 1% agarose and sealed with a coverglass. Images were recorded on a Coolsnap FX CCD camera (Roper Scientific) connected to an Olympus BX60 fluorescence microscope (Japan) fitted with an Olympus U Plan Fl 100 × 1.3NA oil immersion phase contrast objective. YFP or CFP fluorescence was detected, using HQ500/20 and D436/20 excitation filters, Q515LP and 455DCLP dichroic mirrors, and HQ535/30 and D480/40 emission filters, respectively (Chroma Technology Corp.).

Relative Brightness in E. coli. Bacteria were grown to $OD_{600} \approx 0.6$ as described above. Cultures were diluted to $OD_{600} = 0.1$ in triplicate and used to inoculate wells of a flat bottom 96-well plate (Greiner Bio-One, Frickenhausen, Germany) in quadruplicate. Per well, 180 μL of medium containing 0.1 mM IPTG was inoculated with 20 μL of diluted bacteria. Bacteria were grown at 37 °C in the fluorescence microplate reader while shaking. Fluorescence was measured every 5 min as described under "pK_a Measurements".

Transient Transfection HeLa Cells. HeLa cells growing on glass coverslips were transfected with plasmid DNA, using Lipofectamine2000 (Invitrogen, Breda, The Netherlands) according to the manufacturer's protocol. To obtain mixed populations of cells expressing different DNA constructs, cells were transfected separately, trypsinized, and mixed 8 h after transfection. For microscopy, the growth medium was replaced with extracellular-like buffer (140 mM NaCl, 5 mM KCl, 1 mM $CaCl_2$, 1 mM $MgCl_2$, 10 mM glucose, and 20 mM Hepes, pH 7.4).

Fluorescence Brightness in HeLa Cells. HeLa cells growing in tissue culture treated 35 mm dishes were transfected with 0.3 μg of plasmid DNA as described above. Fluorescence imaging was done 18 h posttransfection. For microscopy, the growth medium was replaced with extracellular-like buffer. Fluorescence images were collected using a Coolsnap HQ CCD camera (Roper Scientific) mounted on a Leica MZ FLIII stereofluorescence microscope, fitted with a Planapo 1× objective, a 100 W high pressure Hg lamp for excitation, and excitation and emission filters as described for under "*Localization in E. coli*". Cells were imaged through the bottom of the 35 mm dishes at 3.2× magnification, using exposure times of 1500 ms and 1250 ms for YFP and CFP variants, respectively. For a single experiment, 3 dishes per VFP variant were used and from each dish 6 images were recorded. Single images contained 100−150 cells, and in total between 1800 and 2300 cells were imaged for each VFP variant. The experiment was repeated in triplicate. Fluorescent cells were identified by image processing as follows. Of each image, background fluorescence was subtracted and fluorescent cells were identified as spots more than 100 pixels in size. The fluorescence per cell was calculated as the sum fluorescence divided by the cell size in pixels. The fluorescence brightness of each VFP variant was defined as the average mean fluorescence of all cells. Image processing was done in Matlab 6.1 (The Mathworks, Natick, MA) using the image processing library DIPlib (Pattern Recognition Group, TU Delft, The Netherlands, http://www.ph.tn.tudelft.nl/DIPlib/).

Immunolabeling of HeLa Cells. HeLa cells were fixed with 1% formaldehyde, permeabilized with 0.5% TritonX-100, and blocked with 1% BSA. Incubation with primary antibody against GFP (Molecular Probes) was done overnight at 4 °C, and incubation with Cy5-labeled secondary antibody was done for 30 min at room temperature. Cells were embedded in Mowiol. Fluorescence microscopy was performed using a Zeiss LSM510 confocal laser scanning microscope, implemented on a Zeiss Axiovert100 inverted microscope. Images were aquired using a Zeiss plan Neofluar 40 × 1.3NA, oil-immersion objective. For imaging of YFP, CFP, and Cy5, the 514 and 458 nm argon-laser lines and the 633 nm line of a helium−neon laser were used for excitation. A series of dichroic mirrors was used to divide fluorescence into separate YFP, CFP, and Cy5 channels. Fluorescence was detected through BP530-550 (YFP), BP470-500 (CFP), and LP650 (Cy5) emission filters. To obtain cross-talk-free images, consecutive images were recorded, using a single laser line for excitation and activation of a single detection channel. The intensity of the excitation light was measured to correct for variations in laser power. Colocalization images of VFP fluorescence and Cy5 fluorescence were recorded. For each image the ratio of VFP fluorescence and Cy5 fluorescence was determined by line fitting on the scatterplots of VFP fluorescence intensity versus Cy5 fluorescence intensity. For each VFP variant, the brightness per amount of protein was defined as the average ratio of VFP fluorescence and Cy5 fluorescence.

Fluorescence Lifetime Imaging Microscopy (FLIM). For frequency-domain wide-field FLIM measurements, the FLIM setup as described by Van Munster et al. (*26*) was used. For imaging of CFP and YFP, a helium−cadmium laser (442 nm, 125 mW) or argon-ion laser (514 nm, 150 mW) (Melles-Griot, Carlsbad, CA), a 455DCLP or 525DCXR dichroic mirror, and a D480/40 or HQ545/30 band-pass emission filter (Chroma Technology Corp.) were used, respectively. The frequency of modulation was 75 MHz. Reference phase and modulation were obtained using a reference filter cube reflecting 0.1‰ of the excitation laser light directly onto the detector. FLIM stacks of 12 phase images were acquired with an exposure time of 250−1000 ms per image, depending of the brightness of the samples, using a Zeiss plan Neofluar 40 × 1.3NA, oil-immersion objective. To minimize artifacts due to photobleaching (always <5% for CFP and <10% for YFP), a permutated recording sequence was used (*27*). Software for control, acquisition, processing, and analysis of the data was written in C++, using Matlab 6.1 and the image processing library DIPlib. The FRET efficiency was calculated using the equation

$$E = 1 - \frac{\tau_{DA}}{\tau_D} \tag{5}$$

where τ_{DA} is the donor lifetime of a heterodimer and τ_D is the donor lifetime of the corresponding unfused CFP variant. FRET efficiencies were calculated, based on phase lifetimes.

RESULTS

Construction of Novel CFP and YFP Mutants. Site-directed mutagenesis was used to convert Venus into a cyan fluorescent protein (Table 1). First, a monomeric Venus (mVenus) was made by introducing the mutation A206K to abolish the tendency to dimerize (*18*). Second, mVenus was converted into a cyan fluorescent protein by reversing mutations F46L and T203Y and introducing mutations G65T, Y66W, and N146I. This cyan fluorescent protein was named SCFP1 and contained the common folding mutations not yet present in ECFP (S72A and A175G), as well as mutations V68L and A206K. SCFP2 was made by changing leucine68 back to valine. Finally, H148D and Y145A/H148D were incorporated into SCFP2 to create SCFP3A and SCFP3B, respectively. SYFP2 was created by changing leucine68 in mVenus back to valine.

Spectral Analysis of Fluorescent Proteins. The different VFP variants showed only minor changes in absorbance and emission spectra (Figure 1, Table 2). For previously published VFP variants, the results of our spectral analysis results resembled closely those already reported (see Table S2, Supporting Information). For all optimized YFP variants, the absorbance spectra displayed a slight reduction at 490 nm compared to EYFP(Q69K), while the emission spectra were identical with the emission maximum at 527 nm. The CFP variants displayed a small decrease in absorbance at the secondary maximum (452 nm), and a slight reduction in

Table 1: Overview of the Mutations in YFP and CFP Variants[a]

	mutations
EYFP(Q96K)	S65G V68L Q69K S72A T203Y
Venus	F46L F64L S65G V68L S72A M153T V163A S175G T203Y
mVenus	F46L F64L S65G V68L S72A M153T V163A S175G T203Y A206K
SYFP2	F46L F64L S65G S72A M153T V163A S175G T203Y A206K
ECFP	F64L S65T Y66W N146I M153T V163A
SCFP1	F64L S65T Y66W V68L S72A N146I M153T V163A S175G A206K
SCFP2	F64L S65T Y66W S72A N146I M153T V163A S175G A206K
SCFP3A	F64L S65T Y66W S72A N146I H148D M153T V163A S175G A206K
SCFP3B	F64L S65T Y66W S72A Y145A N146I H148D M153T V163A S175G A206K
Cerulean(A206K)	F64L S65T Y66W S72A Y145A N146I H148D M153T V163A A206K

[a] Annotation based on wtGFP amino acid sequence, GenBank Accession number M62653 (*1*).

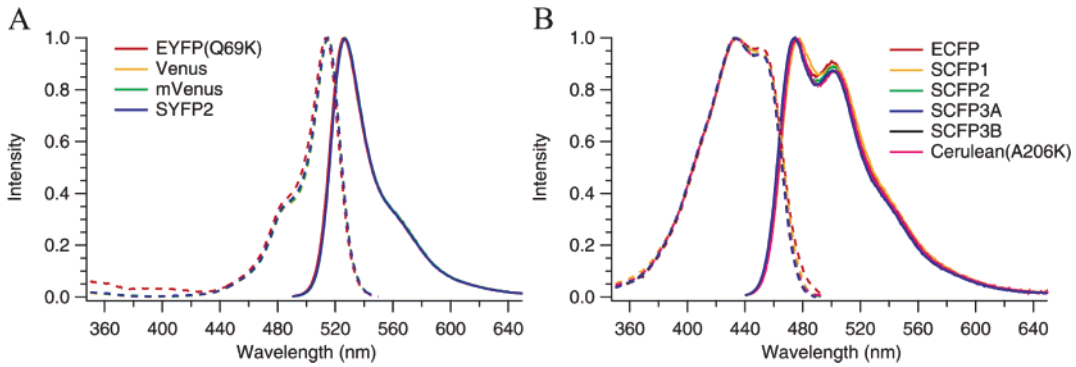

FIGURE 1: Absorbance and emission spectra. Comparison of absorbance (dotted lines) and emission spectra (solid lines) between YFP (A) and CFP (B) variants. Excitation wavelengths were 480 and 430 nm for YFPs and CFPs, respectively. The spectra represent the average of at least 3 measurements from 3 independent protein isolations.

Table 2: Characterization of VFP Variants

				brightness[c]							lifetimes (ns)[e]	
						HeLa						
	$\epsilon \times 10^3$ (λ_{max})[a]	QY (λ_{max})[b]	pK_a	ϵ*QY	*E. coli*	VFP-fluor	immuno-labeling	K_{fold} (10^{-2} s^{-1})	K_{ox} (10^{-4} s^{-1})	τ_{bleach}[d]	phase (φ)	mod
EYFP(Q96K)	72 (514)	0.76 (526)	5.8	1	1	1 ± 0.1	1 ± 0.2	0.4		1	2.8 ± 0.1	3.1 ± 0.1
Venus	110 (515)	0.63 (527)	5.6	1.3	6.5	1.5 ± 0.3	1.3 ± 0.2	1.5	1.7	1.0	2.8 ± 0.1	3.0 ± 0.1
mVenus	105 (515)	0.64 (527)	5.5	1.2	7.5	1.3 ± 0.2	1.4 ± 0.2	2.2	1.6	1.0	2.7 ± 0.1	2.9 ± 0.1
SYFP2	101 (515)	0.68 (527)	6.0	1.3	12.0	1.4 ± 0.1	1.5 ± 0.2	1.0	2.1	0.7	2.9 ± 0.1	3.1 ± 0.1
ECFP	28 (434)	0.36 (474)	4.8	1	1	1 ± 0.1	1 ± 0.2	1.1		1	2.3 ± 0.2	3.0 ± 0.1
SCFP1	29 (434)	0.24 (477)	<3.5	0.7	2.9	0.7 ± 0.1	1.0 ± 0.2	2.7	1.6	1.1	1.5 ± 0.1	2.0 ± 0.1
SCFP2	29 (434)	0.41 (474)	<3.5	1.2	5.0	1.0 ± 0.1	1.2 ± 0.2	1.3	1.5	1.0	2.3 ± 0.1	3.0 ± 0.1
SCFP3A	30 (433)	0.56 (474)	<4.5	1.7	9.0	1.0 ± 0.2	1.5 ± 0.2	1.1	1.4	1.1	2.6 ± 0.1	3.2 ± 0.1
SCFP3B	30 (433)	0.50 (474)	<4.5	1.5	7.6	0.9 ± 0.2	1.1 ± 0.2	1.6		1.2	2.3 ± 0.1	3.1 ± 0.1
Cerulean(A206K)	33 (434)	0.49 (475)	<4.5	1.6	7.4	1.0 ± 0.1	1.3 ± 0.3	1.5		1.1	2.3 ± 0.1	3.1 ± 0.1
Cerulean(206A)											2.2 ± 0.1	2.9 ± 0.1

[a] Extinction coefficient (M^{-1} cm^{-1}) with excitation maximum (nm) in parentheses. [b] Quantum yield with emission maximum (nm) in parentheses. [c] Relative brightness based on quantum yield and extinction coefficient (ϵ*QY) and expression in *E. coli* and HeLa cells. VFP-fluor represents the fluorescence intensity relative to EYFP(Q69K) and ECFP, respectively ($n = 3$). Immunolabeling represents the VFP/Cy5 fluorescence ratio, relative to EYFP(Q69K) and ECFP, respectively ($n = 10$). Numbers indicate mean values and standard deviation. [d] Time needed to bleach 1/e of total fluorescence relative to EYFP(Q69K) or ECFP (higher numbers reflect higher photostability). [e] Fluorescence lifetimes in HeLa cells. Lifetime measurements represent the average and standard deviation of at least 10 measurements, except for SCFP2 ($n = 4$).

fluorescence at the secondary maximum at 500 nm compared to ECFP. These changes were most profound for SCFP3A and SCFP3B, both containing mutation H148D. The emission spectrum of SCFP1 was 3 nm red-shifted (477 nm), but changing leucine68 back to valine returned the emission maximum to 474 nm. The QY of SCFP1 was 0.24 and nearly 30% reduced compared to ECFP (0.36) (Table 2). This QY reduction was most likely caused by leucine68, because changing leucine68 back to valine increased the QY of SCFP2 to 0.41. For SCFP3A the QY was further increased to 0.56 as a result of mutation H148D. A similar effect of this mutation on ECFP QY was described by Rizzo et al. (*17*). Introduction of Y145A in SCFP3B caused a slight decrease in QY as described for Cerulean (*17*); however, we did not observe an increase in extinction coefficient. SCFP3B and Cerulean(A206K) had similar extinction coefficient and QY, and because these VFPs differ by only one point mutation, S175G, we can conclude that S175G has little effect on these properties. Overall only minor changes in extinction coefficient were observed, ranging from 28 000 to 33 000 (Table 2).

Mutations V68L and A206K had little effect on the spectral properties of YFP. Changing leucine68 back to valine in SYFP2 resulted in a slight increase in QY as well

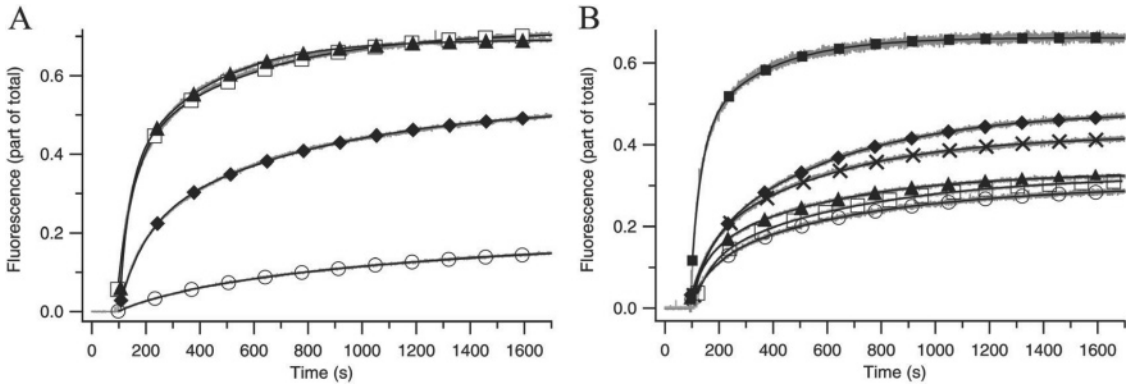

FIGURE 2: Refolding of fluorescent proteins after denaturation. Representative refolding curves with curve fits for the YFP variants (A) EYFP(Q69K) (○), Venus (□), mVenus (▲), and SYFP2 (◆), and for the CFP variants (B) ECFP (○), SCFP1 (■), SCFP2 (▲), SCFP3A (◆), SCFP3B (×), and Cerulean(A206K) (□). Fluorescence intensities are normalized to the fluorescence of an equal amount of native protein.

(Table 2), but the effect was less profound than for the CFP variants. Addition of A206K did not change the QY of mVenus, and neither addition of A206K nor changing leucine68 to valine influenced the extinction coefficient, ranging from 110 000 for Venus to 101 000 for SYFP2 (Table 2).

The fluorescence intensity of fluorescent proteins is pH dependent, and a pK_a well below physiological pH is recommended to prevent artifacts in fluorescence due to pH changes inside cells. Early YFP variants have pK_a values close to pH 7, and hence their fluorescent properties in cells were highly pH dependent. EYFP(Q69K) (*28*) and Venus (*16*) are relatively pH insensitive, and we measured pK_a values of 5.8 and 5.6, respectively (Table 2), slightly lower than reported before (compare Table S2). Changing leucine68 back to valine in SYFP2 increased the pK_a by 0.5 unit. Of the CFP variants, only ECFP displayed a sigmoidal pH dependence (pK_a 4.8). All other CFP variants were insensitive to changes in pH between pH 5.0 and 9.5 (data not shown). As for the YFP variants, V68L reduced the pH sensitivity of SCFP1 compared to ECFP. Introduction of mutation H148D in SCFP3A increased the pK_a by 1 unit, similar to the results observed for GFP(S65T) (*29*).

Bleach Rates. Besides brightness, the photostability of a fluorescent protein is a very important property, because bleaching limits the time a fluorescence signal can be detected. Minor changes in photostability were observed for the CFP variants and none for the YFP variants containing V68L (Table 2). However, changing leucine68 back to valine decreased the relative bleaching time of SYFP2 by 30%. Thus, mutationV68L contributes to the photostability of YFP.

Protein Folding and Chromophore Oxidation. During protein isolation, we observed that protein isolates of VFPs were brightly colored immediately after protein extraction, with the exception of isolates of Venus, mVenus, and SCFP1, which were faintly colored after protein extraction and required overnight incubation to reach vivid coloration. The delay was caused by mutation V68L, since it was absent in SYFP2 and SCFP2. This prompted us to study protein refolding and chromophore oxidation in vitro. For Venus, refolding was approximately 4 times faster compared to EYFP(Q69K) and the percentage of fluorescence recovery also was about 4-fold higher (Figure 2A, Table 2). Addition of A206K in mVenus had little effect on refolding and percentage recovery. Surprisingly, changing leucine68 to valine in SYFP2 decreased the rate of protein refolding by a factor of 2 and reduced the percentage of recovery. This was unexpected, because of the observed delay in fluorescence development for V68L containing VFPs during protein isolation. For SCFP1 the rate of protein refolding increased 2.5 times compared to ECFP and the amount of correctly refolded protein doubled (Figure 2B, Table 2). Again mutation V68L increased the rate and efficiency of refolding, because changing leucine68 back to valine in SCFP2 resulted in a rate and efficiency of refolding similar to those for ECFP. The improvements in protein folding of SCFP1 were less pronounced than for mVenus, probably because ECFP already contained the folding mutations F64L, M153T, and V163A. For SCFP2, SCFP3A, SCFP3B, and Cerulean(A206K) the rate of protein refolding was similar to that for ECFP, but the efficiency was highest for SCFP3A. The rates of chromophore oxidation were similar for all VFPs studied (Table 2).

Localization in E. coli. During protein isolation we found a large portion of GST-EYFP(Q69K) and GST-ECFP in the insoluble fraction. Indeed, GST-EYFP(Q69K) was present in fluorescent spots at the poles of the bacteria, also visible in phase contrast (Figure 3A,B) and likely representing aggregates or inclusion bodies. The fluorescence of the GST-EYFP(Q69K) and GST-ECFP aggregates indicated that, in these inclusion bodies, part of the protein was correctly folded. GST-Venus localized in aggregates but in addition displayed a spotted pattern (Figure 3C). Introduction of A206K resulted in a cytosolic localization for GST-mVenus (Figure 3D), although some barely fluorescent aggregates remained, probably due to the high level of protein expression. GST-ECFP was localized mainly in aggregates as well, despite the presence of folding mutations M153T and V163A (Figure 3E,F). GST-SCFP1 (Figure 3G) and the other GST-SCFP variants were distributed evenly throughout the cytosol, identical to GST-mVenus. Protein aggregates or inclusion bodies generally consist of misfolded protein.

Relative Brightness in E. coli. The brightness of fluorescent proteins in vivo is an important indicator for the quality of a fluorescent protein. Therefore, we measured the time course of fluorescence development in *E. coli* cultures expressing VFP variants as GST-tagged fusion proteins at 37 °C (Figure 4, Table 2). The growth rate of all *E. coli* cultures was similar (data not shown); therefore no correction for bacterial growth was required.

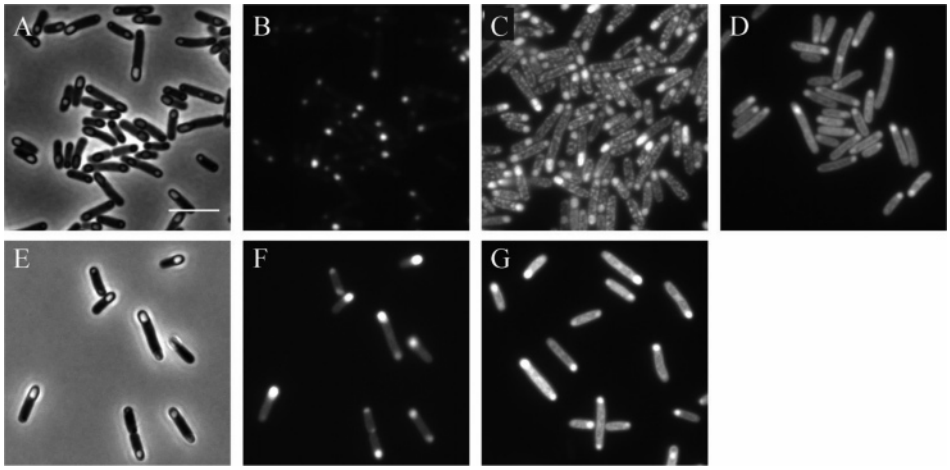

FIGURE 3: Localization of GST-tagged VFP variants in *E. coli*. After 4 h of protein expression, EYFP(Q69K) was present in large spots visible in phase contrast (A) and fluorescence (B). Venus (C) was localized in large spots at the poles of the cell and many smaller spots throughout the cytosol. mVenus (D) was mainly cytosolic. ECFP (E and F) was localized in large spots and to some extent in the cytosol. SCFP1 (G) was present mainly in the cytosol. Scale bar = 5 μm.

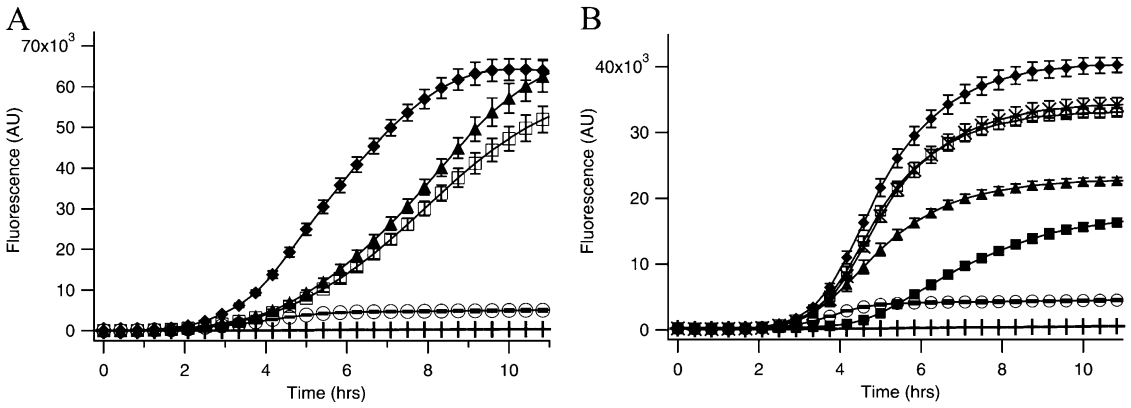

FIGURE 4: Expression of GST-tagged VFP variants in *E. coli* at 37 °C. (A) YFP variants: EYFP(Q69K) (○), Venus (□), mVenus (▲), and SYFP2 (◆). (B) CFP variants: ECFP (○), SCFP1 (■), SCFP2 (▲), SCFP3A (◆), SCFP3B (×), and Cerulean(A206K) (□). Bacteria expressing only the GST-tag (+) were included to measure the levels of autofluorescence. Bars indicate the standard deviation (n = 12). Induction of protein expression was at t = 0 h. Fluorescence is in arbitrary units (AU).

Bacteria expressing GST-EYFP(Q69K) became barely fluorescent. In contrast, *E. coli* expressing GST-Venus developed bright fluorescence and after 9 h were 6.5 times more fluorescent than bacteria expressing GST-EYFP-(Q69K). Fluorescence was elevated further by introduction of A206K in mVenus and by changing leucine68 back to valine in SYFP2. After 9 h, bacteria expressing GST-SYFP2 were most fluorescent and 12 times brighter than GST-EYFP(Q69K). Bacteria expressing GST-ECFP became barely fluorescent, similar to GST-EYFP(Q69K), and fluorescence reached a plateau after approximately 5 h. After 9 h, bacteria expressing GST-SCFP1 became 3 times more fluorescent than those expressing GST-ECFP. Changing leucine68 back to valine increased the brightness of the bacteria 5-fold (compare SCFP2 and ECFP). Addition of H148D increased this brightness even 9-fold (compare SCFP3A and ECFP). Incorporation of Y145A (in SCFP3B) led to a slight decrease in the fluorescent yield of the bacteria. Bacteria expressing Cerulean(A206K) or SCFP3B, both containing Y145A, were equally bright, thus Y145A did not increase the brightness. By comparing SCFP3B and Cerulean(A206K), we concluded that S175G did not affect the fluorescent yield in *E. coli*. Thus SCFP3A, yielding 9 times more fluorescence than ECFP, was the brightest CFP variant in *E. coli*. Measuring the time course of fluorescence development revealed a delay for all CFP and YFP variants containing mutation V68L, as also observed during protein isolation.

Relative Brightness in HeLa Cells. Differences in fluorescence intensity were also observed upon expression of the VFP variants in HeLa cells, although these variations were less pronounced than in bacteria. For the YFP variants, the differences in HeLa cells (Table 2) correlated well with the intrinsic brightness (i.e. the product of extinction coefficient and QY) of the purified recombinant protein. Upon expression of the CFP variants, only a decrease in total fluorescence for HeLa cells expressing SCFP1 was observed, in agreement with its reduced QY. In order to correct for differences in expression levels (if any), we also performed immunolabeling studies using Cy5-labeled antibodies. The VFP fluorescence intensity was compared to the (Cy5) immunofluorescence so that the fluorescence per expressed protein in HeLa cells (i.e. native fluorescent and denatured or immature nonfluorescent protein) could be determined. For all VFP variants, a linear correlation between VFP and Cy5 fluorescence intensity was observed. For the SYFP variants, the VFP/Cy5 fluorescence ratios closely correlated with the differences in average fluorescence intensity (Table 2). For the SCFP variants, SCFP3A displayed a clearly improved VFP/Cy5 ratio. Again, the VFP/Cy5 ratio correlated well with the intrinsic brightness (Table 2). Because

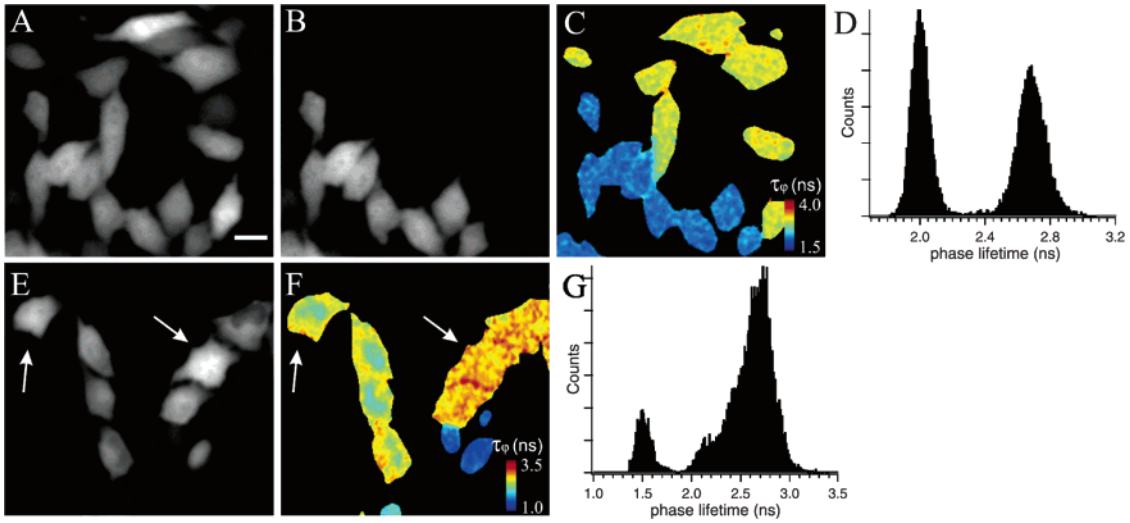

FIGURE 5: FRET-FLIM and dual-lifetime imaging in HeLa cells. (A−D) Cells expressing SYFP2−SCFP3A dimer show a decreased fluorescence lifetime, as a result of FRET. Cells expressing SYFP2−SCFP3A are recognized by the presence of both CFP fluorescence (A) and YFP fluorescence (B) and by the strong decrease in phase lifetime (C). (D) Phase-lifetime histogram of panel C, showing 2 completely separated lifetime populations with a large lifetime difference of 0.7 ns. (E−G) Dual-lifetime imaging with SCFP1 and SCFP3A. (E) Cells expressing SCFP1−NLS, SCFP3A−NES, or both cannot be discriminated based on fluorescence intensity (compare cells indicated by arrows). (F) Phase-lifetime image showing the presence of the 3 cell populations. (G) Phase-lifetime histogram of panel F showing the lifetime distribution. Scale bar = 10 μm.

SCFP3A and ECFP gave nearly identical overall fluorescence in HeLa cells, it appears that SCFP3A expression levels in HeLa cells were somewhat reduced.

Fluorescence Lifetime Measurements. ECFP/EYFP is a widely used donor/acceptor pair for VFP-based FRET applications (*10*). One of the most robust techniques for quantifying FRET in living cells is FLIM (*30*). However, because of the multiexponential lifetime decay, it is hard to obtain quantitative data on protein distributions from FRET measurements, using ECFP (*22*, *31*). Rizzo et al. (*17*) created Cerulean, a bright CFP variant with a fluorescence lifetime best fitted by a monoexponential decay as a result of a single point mutation H148D. We measured the fluorescence lifetimes of fluorescent proteins expressed in HeLa cells, using frequency-domain FLIM (*27*), and lifetimes were calculated based on the phase shift (τ_φ) and change in modulation depth (τ_{mod}). In the case of a single-exponential lifetime decay, τ_φ equals τ_{mod}, whereas for multiexponential decays $\tau_\varphi < \tau_{mod}$ (*12*, *22*, *32*). In this way single-exponential and multiexponential decays are very easily discriminated in frequency-domain FLIM even working at a single modulation frequency.

All YFP variants had comparable lifetimes of about 3 ns, and τ_φ and τ_{mod} were very similar, indicating a nearly monoexponential lifetime decay (Table 2), as observed before (Table S2) (*27*, *33*). In contrast, τ_φ and τ_{mod} lifetimes of all CFP variants differed considerably (Table 2). Compared to ECFP (τ_φ = 2.3 ns, τ_{mod} = 3.0 ns), a decrease in lifetime was observed of approximately 1 ns for SCFP1 (τ_φ = 1.5 ns, τ_{mod} = 2.0 ns) and an increase of about 0.3 ns for SCFP3A (τ_φ = 2.6 ns, τ_{mod} = 3.2 ns). These changes correlated well with the fluorescence quantum yields. The decrease in lifetime of SCFP1 was due to mutation V68L, because changing leucine68 back to valine in SCFP2 yielded a lifetime identical to that of ECFP. Also for Cerulean-(A206K), a clear difference between τ_φ and τ_{mod} was observed with $\tau_\varphi < \tau_{mod}$, demonstrating multiexponential fluorescence decay. To exclude the possibility that mutation A206K in Cerulean(A206k) disrupted the monoexponential lifetime decay, we removed this mutation to create Cerulean as described by Rizzo et al. (*17*). Nevertheless mutation A206K had a negligible effect on the fluorescence lifetime and the difference between τ_φ and τ_{mod} persisted.

Table 3: FRET Efficiency of Heterodimers[a]

	τ_D (ns)	τ_{DA} (ns)	$\Delta\tau$ (ns)	E (%)
EYFP(Q69K)−ECFP	2.23 ± 0.09	1.67 ± 0.04	0.56 ± 0.12	25.0 ± 4.4
SYFP2−ECFP	2.22 ± 0.06	1.69 ± 0.04	0.53 ± 0.08	23.8 ± 2.9
SYFP2−SCFP3A	2.64 ± 0.11	1.93 ± 0.07	0.70 ± 0.10	26.5 ± 2.9

[a] FRET efficiency (E) based on the phase lifetimes of HeLa cells expressing either plain donor CFP (τ_D) or a heterodimer (τ_{DA}), using eq 5. Values represent the average and standard deviation (n = 11).

FRET Efficiency of YFP−CFP Dimers. To determine the best CFP/YFP pair for FRET experiments, the FRET efficiency of tandem fusions of YFP and CFP variants was measured. In each heterodimer, donor and acceptor were separated by a flexible linker of 12 amino acids. FRET efficiencies were determined by the lifetime decrease in HeLa cells expressing a heterodimer, compared to cells expressing only donor CFP (Figure 5A,B). Cells expressing a tandem YFP−CFP fusion were identified by the presence of YFP fluorescence and by the decrease in fluorescence lifetime (Figure 5A−D). The change in lifetime ($\Delta\tau$) due to FRET was largest for SYFP2−SCFP3A (0.70 ± 0.10 ns), followed by EYFP−ECFP (0.56 ± 0.12 ns) and SYFP2−ECFP (0.53 ± 0.08 ns) (Table 3). However, the FRET efficiency of SYFP2−SCFP3A did not increase.

Dual-Lifetime Imaging with SCFP1 and SCFP3A. SCFP1 and SCFP3A are spectrally identical and therefore cannot be distinguished based on fluorescence. However, the large difference in fluorescence lifetime enabled discrimination by FLIM. HeLa cells expressing SCFP1−NLS, SCFP3A−NES, or both could not be distinguished, based on localization of fluorescence (see cells indicated by arrows, Figure 5E). In contrast, the 3 cell populations were readily identified from the lifetime image (Figure 5F). Even cells expressing both

fluorescent proteins were identified, by the difference in fluorescence lifetime in the nucleus compared to the cytoplasm. These experiments provide, to our knowledge, the first example of dual-lifetime imaging with spectrally identical (cyan) fluorescent proteins in living cells. Contrast by FLIM has been reported before by Pepperkok et al.(*33*); however, this involved spectrally similar, but not identical (e.g. CFP, GFP, and YFP), fluorescent proteins.

DISCUSSION

The aim of this research was to study the effects of specific mutations on the spectroscopic properties and folding characteristics of CFP and YFP and create super yellow and cyan fluorescent proteins for use in *E. coli* and mammalian cells. The effective brightness of fluorescent proteins in cells depends not only on spectroscopic properties, such as extinction coefficient and quantum yield, but also on the rate and efficiency of protein folding and chromophore formation. In other words, not only is the fluorescence per molecule important but also the fraction of correctly folded fluorescent molecules produced is critical. This is best exemplified by the results for SCFP1. Based on extinction coefficient and quantum yield, a 30% reduction in fluorescence brightness relative to ECFP was expected for SCFP1, due to the presence of V68L. However, *E. coli* cultures expressing SCFP1 were 3-fold brighter than those expressing ECFP, because mutations S72A, S175G, and A206K greatly improved protein folding and solubility and apparently enabled more protein to become fluorescent.

When using fluorescent proteins, especially when studying protein−protein interaction, it is important that the fluorescent proteins do not interact themselves, because this can give rise to artifacts in localization and false positive interactions. VFP variants were expressed as GST-fusion proteins in *E. coli*. GST (glutathione S-transferase) is known to form homodimers ($K_d < 1\ \mu M$) in the cytosol of *E. coli* (*34*, *35*). If a VFP has the tendency to dimerize, the presence of two interaction sites in each GST-VFP molecule can lead to oligomerization and hence induce aggregation. Aggregation of GST-VFP proteins can therefore indicate inefficient protein folding, as well as a tendency of the VFP to dimerize. Protein aggregates or inclusion bodies, as observed for EYFP(Q69K) and ECFP, generally consist of misfolded protein. Since the inclusion bodies were fluorescent, this means that besides aggregated misfolded VFPs they also contained correctly folded but aggregated VFPs. This explains the overall reduced fluorescence in these bacteria and the visibility of the inclusion bodies by fluorescence microscopy.

Comparison of the localization of GST-EYFP(Q69K) and GST-ECFP to that of GST-mVenus and GST-SCFP2 clearly showed that mutations F64L, S72A, M153T, V163A, S175G, and A206K reduce aggregation of both cyan and yellow fluorescent GST-fusion proteins. The significance of A206K was clear from the bacterial expression of YFP variants, where introduction of the single mutation A206K into Venus was required for a true cytosolic localization.

Because folding of fluorescent proteins in *E. coli* is inefficient (*36*), fluorescence brightness greatly benefits from mutations that facilitate protein folding. Eukaryotic cells on the other hand can efficiently express and fold fluorescent proteins, making folding mutations less necessary. The improvements in apparent brightness of the VFPs in eukaryotic cells were therefore much less pronounced than in bacteria. Interestingly, the relative brightness of mammalian cells expressing the VFP variants was correlated with the intrinsic brightness derived from the spectral properties of purified proteins. This indeed indicated that folding and maturation efficiencies of the different VFP variants are roughly the same in mammalian cells.

Mutation V68L delayed fluorescence development in bacteria; however, we have a paradox, as protein folding in vitro was accelerated. Chromophore formation requires proper protein folding, followed by chromophore cyclization, oxidation, and dehydration. The precise sequence of events in chromophore maturation is still under debate (*37*, *38*). Our results indicate that V68L increases the rate of protein refolding of denatured protein and does not affect the rate of chromophore oxidation; therefore we assume that replacing valine68 for the bulkier leucine causes a delay in fluorescence development by hindering chromophore cyclization. However, recent studies on EGFP chromophore formation have shown that backbone cyclization is an energetically unfavorable reaction and chromophore oxidation might be required for ring stabilization (*37*). If this is true, then chromophore reduction results in ring opening and consequently the kinetics of chromophore reoxidation represent both ring closure and oxidation. Because the kinetics of fluorescence recovery after protein denaturation with chromophore reduction are similar for all SVFPs studied, this would disfavor an effect of V68L on backbone cyclization. Alternatively, the paradox might be explained by the absence of certain cytosolic (protein) compounds in the in vitro refolding assays, that influence folding and maturation in vivo. Although interesting, the further exploration of these compounds is beyond the scope of this article. In any case, our data suggest that the kinetics, observed during in vitro refolding/reoxidation assays, sometimes only partially reflect VFP maturation in living cells.

The fluorescence lifetime decay is directly related to the quantum yield of the chromophore (*39*). This correlation was clear from the lifetime measurements of all VFP variants. The low quantum yield of SCFP1 resulted in a short fluorescence lifetime of 1.5 ns. And the high quantum yield of SCFP3A increased the fluorescence lifetime to 2.6 ns. The difference between τ_φ and τ_{mod} for all CFP variants clearly shows that none of these fluorescent proteins, Cerulean included, have a monoexponential lifetime decay. Therefore we must conclude that mutation H148D is not sufficient to create a true monoexponential lifetime decay. The reason for the discrepancy with the published data is unclear to us, but might be caused by the different experimental setups, i.e. time-correlated single-photon counting spectroscopy versus frequency-domain FLIM, and the difference in excitation wavelength, i.e. 442 nm versus 425 nm by Rizzo et al. Although the lifetime decay of Cerulean is fitted best by a monoexponential decay, this does not necessarily mean the lifetime decay is actually monoexponential. Multiexponential lifetime decay for Cerulean, both in frequency- and time-domain FLIM, has been found by others as well (P. I. Bastiaens, K. Jalink, and F. S. Wouters, personal communication[2]).

Based on eqs 3 and 4 and a measured FRET efficiency of 25% for EYFP(Q69K)−ECFP, the FRET efficiency of

SYFP2−SCFP3A was expected to be 38%. However the FRET efficiency of SYFP−SCFP3A was similar to that of EYFP(Q69K)−ECFP. This inconsistency was most likely caused by the tendency of EYFP(Q69K) and ECFP to dimerize. As shown by Zacharias et al. (*18*), affinity between donor and acceptor will favor a conformation in which donor and acceptor are in very close proximity, thereby reducing the average distance between donor and acceptor and in this way increasing the FRET efficiency. Furthermore, in such a preferred conformation, the assumption of $\kappa^2 = 2/3$ in eq 2 is not valid. Depending on the actual relative orientation of the donor and acceptor dipole moments, in the preferred conformation, κ^2 can vary between 0 and 4, making the FRET efficiency unpredictable. This orientation effect has been exploited by Nagai et al. to improve the dynamic range of yellow cameleons (*40*), by using circular permutated acceptors with markedly different dipole moment orientations. Hence, the absence of an increase in FRET efficiency of SYFP2−SCFP3A despite the high intrinsic brightness of both VFPs, compared to EYFP(Q69K)−ECFP, is probably the result of the loss in their tendency to dimerize, causing a less favorable orientation/distance of the tandem fusion for FRET. If orientation effects can be ignored ($\kappa^2 = 2/3$ can be assumed), our spectroscopic evaluation yields an $R_0 = 5.4$ nm for the SCFP3A/SYFP2 FRET pair, being significantly higher than that of ECFP/EYFP(Q69K) ($R_0 = 4.7$ nm). Hence, for interaction studies, SCFP3A/SYFP2 is the preferred donor/acceptor pair.

The decrease in QY of SCFP1 was unfavorable for the fluorescence brightness; however, the associated decrease in fluorescence lifetime together with the increased lifetime of SCFP3A enabled separate detection of SCFP1 and SCFP3A by FLIM. The main advantage of dual-lifetime FLIM with spectrally identical fluorescent proteins is the ability to do multiparameter imaging, without using additional spectral channels (*41*).

With SCFP3A and SYFP2 we have created a set of improved monomeric fluorescent proteins with optimized folding and maturation. These properties make SCFP3A and SYFP2 superior to other cyan and yellow VFP variants, presently available for FRET or dual-color labeling. Furthermore, with the development of SCFP1 and SCFP3A, we show it is possible to detect two spectrally identical cyan fluorescent proteins without the requirement of quenching processes like FRET.

ACKNOWLEDGMENT

We thank Dr. A. Miyawaki (Brain Science Institute, RIKEN, Saitama, Japan) for the pCS2+ Venus plasmid, Dr. D. W. Piston (Vanderbilt University Medical Centre, Nashville, TN) for the pCerulean(A206K)-C1 plasmid, and M. Luijsterburg for helpful advice and providing the Cy5-labeled antibody. We sincerely thank W. Takkenberg (deceased) for technical assistance.

[2] Personal communication: P. I. Bastiaens, Cell Biology and Biophysics Program, EMBL, Heidelberg, Germany; K. Jalink, Division of Cell Biology, The Netherlands Cancer Institute, Amsterdam, The Netherlands; F. S. Wouters, Cell Biophysics Group, European Neuroscience Institute, Göttingen, Germany.

SUPPORTING INFORMATION AVAILABLE

Oligonucleotides used for site-directed mutagenesis are listed in Table S1. Spectroscopic data from literature is listed in Table S2. This material is available free of charge via the Internet at http://pubs.acs.org.

REFERENCES

1. Prasher, D. C., Eckenrode, V. K., Ward, W. W., Prendergast, F. G., and Cormier, M. J. (1992) *Gene 111*, 229−233.
2. Chalfie, M., Tu, Y., Euskirchen, G., Ward, W. W., and Prasher, D. C. (1994) *Science 263*, 802−805.
3. Tsien, R. Y. (1998) *Annu. Rev. Biochem. 67*, 509−544.
4. Cubitt, A. B., Woollenweber, L. A., and Heim, R. (1999) *Methods Cell Biol. 58*, 19−30.
5. Siemering, K. R., Golbik, R., Sever, R., and Haseloff, J. (1996) *Curr. Biol. 6*, 1653−1663.
6. Fukuda, H., Arai, M., and Kuwajima, K. (2000) *Biochemistry 39*, 12025−12032.
7. Patterson, G. H., Knobel, S. M., Sharif, W. D., Kain, S. R., and Piston, D. W. (1997) *Biophys. J. 73*, 2782−2790.
8. Cormack, B. P., Valdivia, R. H., and Falkow, S. (1996) *Gene 173*, 33−38.
9. Patterson, G., Day, R. N., and Piston, D. (2001) *J. Cell Sci. 114*, 837−838.
10. Zhang, J., Campbell, R. E., Ting, A. Y., and Tsien, R. Y. (2002) *Nat. Rev. Mol. Cell Biol. 3*, 906−918.
11. Förster, T. (1948) *Ann. Phys. 2*, 55−75.
12. Patterson, G. H., Piston, D. W., and Barisas, B. G. (2000) *Anal. Biochem. 284*, 438−440.
13. Stryer, L. (1978) *Annu. Rev. Biochem. 47*, 819−846.
14. Clegg, R. M. (1996) in *Fluorescence Imaging Spectroscopy and Microscopy* (Wang, X. F., and Herman, B., Eds.) pp 179−252, John Wiley & Sons, Inc.
15. van der Meer, B. W. (2002) *J. Biotechnol. 82*, 181−196.
16. Nagai, T., Ibata, K., Park, E. S., Kubota, M., Mikoshiba, K., and Miyawaki, A. (2002) *Nat. Biotechnol. 20*, 87−90.
17. Rizzo, M. A., Springer, G. H., Granada, B., and Piston, D. W. (2004) *Nat. Biotechnol. 22*, 445−449.
18. Zacharias, D. A., Violin, J. D., Newton, A. C., and Tsien, R. Y. (2002) *Science 296*, 913−916.
19. Sambrook, J., and Russel, D. W. (2001) *Molecular cloning: A laboratory Manual*, 3rd ed., Cold Spring Harbor Laboratory Press, Cold Spring Harbor, NY.
20. Sawano, A., and Miyawaki, A. (2000) *Nucleic Acids Res. 28*, E78.
21. Guan, K. L., and Dixon, J. E. (1991) *Anal. Biochem. 192*, 262−267.
22. Vermeer, J. E., Van Munster, E. B., Vischer, N. O., and Gadella, T. W., Jr. (2004) *J. Microsc. 214*, 190−200.
23. Velapoldi, R. A., and Tonnesen, H. H. (2004) *J. Fluorescence 14*, 465−472.
24. Zwier, J. M., Van Rooij, G. J., Hofstraat, J. W., and Brakenhoff, G. J. (2004) *J. Microsc. 216*, 15−24.
25. Reid, B. G., and Flynn, G. C. (1997) *Biochemistry 36*, 6786−6791.
26. Van Munster, E. B., and Gadella, T. W., Jr. (2004) *J. Microsc. 213*, 29−38.
27. van Munster, E. B., and Gadella, T. W., Jr. (2004) *Cytometry 58A*, 185−194.
28. Miyawaki, A., Griesbeck, O., Heim, R., and Tsien, R. Y. (1999) *Proc. Natl. Acad. Sci. U.S.A. 96*, 2135−2140.
29. Elsliger, M. A., Wachter, R. M., Hanson, G. T., Kallio, K., and Remington, S. J. (1999) *Biochemistry 38*, 5296−5301.
30. Squire, A., Verveer, P. J., and Bastiaens, P. I. (2000) *J. Microsc. 197* (Part 2), 136−149.
31. Tramier, M., Gautier, I., Piolot, T., Ravalet, S., Kemnitz, K., Coppey, J., Durieux, C., Mignotte, V., and Coppey-Moisan, M. (2002) *Biophys. J. 83*, 3570−3577.
32. Gadella, T. W., Jr., Jovin, T. M., and Clegg, R. M. (1993) *Biophys. Chem. 48*, 221−239.
33. Pepperkok, R., Squire, A., Geley, S., and Bastiaens, P. I. (1999) *Curr. Biol. 9*, 269−272.
34. Lim, K., Ho, J. X., Keeling, K., Gilliland, G. L., Ji, X., Ruker, F., and Carter, D. C. (1994) *Protein Sci. 3*, 2233−2244.

35. Riley, L. G., Ralston, G. B., and Weiss, A. S. (1996) *Protein Eng. 9*, 223−230.
36. Chang, H. C., Kaiser, C. M., Hartl, F. U., and Barral, J. M. (2005) *J. Mol. Biol. 353*, 397−409.
37. Rosenow, M. A., Huffman, H. A., Phail, M. E., and Wachter, R. M. (2004) *Biochemistry 43*, 4464−4472.
38. Barondeau, D. P., Kassmann, C. J., Tainer, J. A., and Getzoff, E. D. (2005) *Biochemistry 44*, 1960−1970.
39. Lakowicz, J. R. (1999) *Principles of fluorescence spectroscopy*, 2nd ed., Kluwer Acadamic/Plenum Publishers, New York.
40. Nagai, T., Yamada, S., Tominaga, T., Ichikawa, M., and Miyawaki, A. (2004) *Proc. Natl. Acad. Sci. U.S.A. 101*, 10554−10559.
41. Schultz, C., Schleifenbaum, A., Goedhart, J., and Gadella, T. W., Jr. (2005) *ChemBioChem 6*, 1323−1330.

BI0516273